Phase diagram of a two-dimensional lattice-gas model of oxygen ordering in $YBa_2Cu_3O_z$ with realistic interactions

D. J. Liu and T. L. Einstein
Department of Physics, University of Maryland, College Park, Maryland 20742

P. A. Sterne
Department of Physics, University of California, Davis, California 95616
and Lawrence Livermore National Laboratory, Livermore, California 94551

L. T. Wille
Department of Physics, Florida Atlantic University, Boca Raton, Florida 33431
(Received 18 May 1995)

We have determined a first-principles temperature-composition phase diagram describing the ordering of oxygen atoms in the "chain" layers of $YBa_2Cu_3O_z$. The calculations are based on a transfer-matrix finite-size-scaling study of a two-dimensional lattice-gas Hamiltonian (the asymmetric next-nearest-neighbor Ising [ASYNNNI] model). The interaction parameters are obtained from *ab initio* electronic structure calculations. The resulting phase diagram compares favorably with experiment. We analyze its sensitivity to the relative size of the interactions. We also show that the addition of a third-neighbor interaction has a minimal effect on the phase boundaries. Based on these results, we assess the applicability of the ASYNNNI model to $YBa_2Cu_3O_z$.

I. INTRODUCTION

Understanding the electronic and structural properties of oxides presents a major theoretical challenge. In addition to possessing various types of electronic and ionic disorder, many oxides are nonstoichiometric, i.e., they exhibit a continuous range of compositions without major structural changes.[1] This is due to the ability of these materials to incorporate concentration changes by forming defects that remain largely disordered. At large defect concentrations, new phases may form with accompanying structural changes. Examples range from relatively simple transition metal oxides, such as $Fe_{1-x}O$ and TiO_{2-x}, to more complex systems such as spinels, garnets, and perovskites. The high-temperature superconductor $YBa_2Cu_3O_z$ belongs to the latter family and displays rich structural behavior.[2] The stoichiometric index z in this compound ranges from 7.0 to close to 6.0. At high temperature, oxygen/vacancy sites in the Cu-O basal plane are randomly populated and the material has tetragonal symmetry. This nonsuperconducting phase will be referred to as Tetra. As the temperature is reduced, the oxygen atoms order into Cu-O chains. This breaks the tetragonal fourfold symmetry, leading to superconducting orthorhombic structures. The OrthoI phase occurs near $z = 7.0$, with Cu-O chains in each unit cell. In addition, an OrthoII phase forms around $z = 6.5$, with a structure derived from that of OrthoI by removing the oxygens in every second chain. OrthoI and OrthoII are commonly believed to be associated with the 90 K and 60 K plateaus in T_c. These plateaus are thought to be due to the oxygen ordering in the basal plane which provides a source of holes for the superconducting CuO_2 planes.[3] In order to optimize the material's superconducting characteristics, one should understand clearly the temperature-composition phase diagram as well as the nature of various metastable phases. These issues have therefore received considerable study, both theoretical and experimental.

The most frequently used model is the two-dimensional asymmetric next-nearest-neighbor Ising (ASYNNNI) model,[4] based on a square lattice with a nearest-neighbor (NN) interaction V_1 and two types of next-nearest-neighbor (NNN) interactions V_2 and V_3. This anisotropy results from the fact that Cu atoms are present in the V_2 NNN bonds, but not in the V_3 NNN bonds. The ASYNNNI model contains the OrthoI and OrthoII structures as ground states for appropriate ranges of these interactions[5] and it provides a remarkably accurate description of the phase diagram.[6–19] Moreover, this model has also been used to account for kinetic phenomena in $YBa_2Cu_3O_z$ such as the room-temperature annealing of quenched material.[20] In spite of its success in describing these material properties, the model does have limitations. For example, chemical potential isotherms[21] and partial molar quantities[22] appear to be described poorly.

The ASYNNNI model omits longer-range interactions which could stabilize other chain-ordered phases.[23,24] However, such structures have only been observed in small patches within a matrix of one of the major phases (OrthoI, OrthoII, or Tetra),[25] and it is therefore unclear if they are thermodynamically stable. While some further extensions of the model have been proposed to explain a number of minor features,[26–30] the basic ASYNNNI model is appealing because only three parameters are used and these may be computed from first-

0163-1829/95/52(13)/9784(9)/$06.00

principles. We emphasize that all phases that have been observed unambiguously in experiments are contained within the ASYNNNI Hamiltonian.

The transfer-matrix finite-size-scaling (TMFSS) method has proven to be a reliable and accurate technique to calculate the phase diagram of two-dimensional models in general and the ASYNNNI model in particular.[8,10,14] In this work, we replace the canonical interactions used in previous studies[8,10] by realistic values obtained from first-principles electronic structure calculations.[31–33] We also investigate the sensitivity of the phase diagram to changes in interaction parameters and examine the effects of including interactions beyond NNN.

The remainder of this paper is organized as follows. Section II describes the ASYNNNI model, discusses its limitations and underlying assumptions, and gives a brief overview of previous work relevant to the present study. Section III outlines the application of the TMFSS method to the problem at hand, while Sec. IV presents our results for the present interaction parameters within the ASYNNNI model as well as for hypothetical further-neighbor interactions. These findings are analyzed and compared to other theoretical and experimental work. Finally, Sec. V contains a summary and some concluding remarks.

II. MODEL

We assume that the Cu-O basal plane may be described by a two-dimensional lattice-gas model, in which the oxygen atoms can occupy sites on a square lattice and have pairwise interactions. The Hamiltonian for this system can be written in either Ising form,

$$\mathcal{H} = -H\sum_i \sigma_i + V_1 \sum_{\mathrm{NN}} \sigma_i\sigma_j + V_2 \sum_{\mathrm{NNN}}{}' \sigma_i\sigma_j + V_3 \sum_{\mathrm{NNN}}{}'' \sigma_i\sigma_j + V_4 \sum_{\mathrm{3rd}} \sigma_i\sigma_j + \cdots, \quad (1)$$

or in the lattice-gas form,

$$\mathcal{H} = -\mu\sum_i n_i + E_1 \sum_{\mathrm{NN}} n_i n_j + E_2 \sum_{\mathrm{NNN}}{}' n_i n_j + E_3 \sum_{\mathrm{NNN}}{}'' n_i n_j + E_4 \sum_{\mathrm{3rd}} n_i n_j + \cdots, \quad (2)$$

where the Ising spin σ_i takes the value 1 (-1), and the lattice-gas occupation number n_i takes the value 1 (0), when there is (is not) an oxygen atom on site i. The model was originally couched in the Ising form,[4] but the lattice-gas form is equivalent and is more natural for transfer-matrix calculations.[8,14] Since most of the literature uses the Ising formulation, we follow that convention here. The V_i's are effective pair interactions (EPI's): V_1 is the NN interaction, V_2 is the NNN interaction through a Cu atom, V_3 is the NNN interaction between sites with no intervening Cu atom, and V_4 is the third-nearest-neighbor interaction. If terms from V_4 onwards are neglected, the Hamiltonian (1) reduces to that of the ASYNNNI model. Since $\sigma_i = 2n_i - 1$, we see easily that $V_m = E_m/4$; furthermore, the chemical potential is related to the effective magnetic field by $\mu = 2H + 4\gamma_1 V_1 + 4\gamma_2 V_2 + 4\gamma_3 V_3 + 4\gamma_4 V_4 + \cdots$, where γ_m is the number of m-type bonds per site ($\gamma_1 = \gamma_4 = 4, \gamma_2 = \gamma_3 = 2$).

There are three major assumptions in the model given by Eq. (1). First it is a strictly two-dimensional model: only a single basal plane is considered, interactions between basal planes are neglected and the apical oxygen sites are fully occupied. Second, the oxygen atoms reside on a rigid, square lattice. One neglects the rectangular distortion associated with the difference in length of the two NNN bonds; thermal lattice expansion is also ignored. Third, only concentration-independent pair interactions are considered: effective cluster interactions that may in principle be present are taken to be negligible and the EPI's are assumed to be independent of oxygen content and temperature. In the ASYNNNI model the additional assumption is made that EPI's beyond NNN are also negligible.

Figure 1 illustrates the interactions between oxygen sites used in the Hamiltonian of Eq. (1). Also shown are

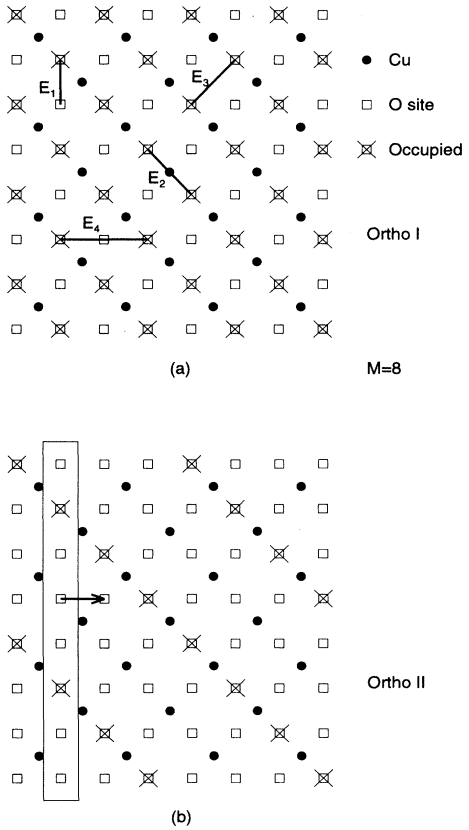

FIG. 1. The two ordered phases and interactions of the lattice-gas model for oxygen atoms on a square lattice. Open squares denote oxygen lattice sites; those with ×'s are occupied. Dots denote copper atoms. (a) The orthorhombic (OrthoI) phase. (b) The double-cell (OrthoII) phase. In (a) the interactions of the lattice-gas model are indicated, while in (b) the $M = 8$ strips and the transfer matrices connecting neighboring strips are indicated.

the two observed ordered structures, OrthoI and OrthoII, with oxygen concentrations $c \equiv \langle n_i \rangle = 1/2$ and $c = 1/4$, respectively. Neglecting interactions beyond NNN, the parameter choice is restricted by the conditions $V_1 > 0$, $V_2 < 0$, and $0 < V_3 < V_1$, so that the two orthorhombic structures are the ground states at $c = 1/2$ and $c = 1/4$.[5]

"Canonical" values, $V_1 > 0, V_2 = -V_3 = -(1/2)V_1$, were used to calculate the phase diagram using the cluster variation method[6,7] (CVM) and related mean-field techniques,[13,15,19] Monte Carlo simulations,[10–12,16,17] transfer-matrix finite-size scaling,[8,10,14] and low-temperature series expansions.[18] All transitions in the ASYNNNI model are second order, although the CVM erroneously predicts a first-order transition along part of the OrthoII-Tetra phase boundary. This is an artefact of the mean-field approximation and is absent in the more accurate statistical mechanical treatments.[8,10,11,14,16,18] For a two-dimensional lattice-gas model with limited-range interactions, the transfer-matrix method yields a better estimation of the phase boundary than other methods, but it becomes unfeasible for long-range interactions. The simplest mean-field theories are able to handle such interactions, but their neglect of fluctuations leads to qualitative and quantitative errors in two-dimensional systems. All other techniques also have trouble with such long-range interactions.

A number of authors used a variety of approaches to determine a more realistic set of EPI's. Sterne and Wille[31,32] computed a parameter set from first-principles total energy calculations which provided a nonempirical phase diagram in excellent agreement with experiment.[9,14,31,32] Poulsen *et al.*[12] obtained a set of EPI's by fitting Monte Carlo calculations of the ASYNNNI model to neutron powder diffraction data. Keeping the ratios fixed, the group subsequently[17] scaled up the interactions by 26%. Hilton *et al.*[14] deduced a set of EPI's by fitting the results of TMFSS calculations to several experiments. Both groups found values that are in reasonable agreement with the first-principles values, but show some quantitative differences.

Extensions to the basic ASYNNNI Hamiltonian have been proposed to account for recent experimental results. The effect of electron spin and charge degrees of freedom[21] can be included by modifying the entropy expression of the free energy, which enables a better description of the thermodynamic response function. Also, elastic strain interactions and the associated orthorhombic distortion[28–30] have been invoked to explain the experimentally observed first-order transitions, while others[26] rationalize this effect in terms of weakly attractive long-range interactions. Elastic interactions in a model that allows atomic displacements also produce as metastable or transient inclusions[29,30] other ordered structures that have been experimentally obtained, notably the $\sqrt{2} \times \sqrt{2}$ and $2\sqrt{2} \times 2\sqrt{2}$ superstructures.[34,35] Long-range interactions[23,24,36–39] will stabilize other chain-ordered structures with unit cells that are a multiple of that of OrthoI, and for some values[38,39] even stabilize the $\sqrt{2}$ structures as true ground states of a rigid-lattice Hamiltonian. However, most authors[34] believe that these $\sqrt{2}$ structures are not thermodynamically stable and are the result of elastic deformations. Such states have also been obtained in a model that includes strain terms in the Hamiltonian.[40] Out-of-plane interactions with the apical oxygen sites have been added to the ASYNNNI model[27] in order to describe the depopulation of these sites at low oxygen contents. In the present paper the majority of the calculations have been restricted to the original ASYNNNI model, except that the effects of a repulsive V_4 term have also been considered.

III. METHOD

In the transfer-matrix method, the lattice is approximated by an $M \times \infty$ lattice with periodic boundary conditions in the finite direction (i.e., an $M \times \infty$ cylindrical surface). The actual transfer matrix accounts for the interactions due to a strip M sites wide. One then iterates this matrix to account for all sites on the cylinder. The principal directions of the cylinder should respect the symmetries of all the phases to insure the most rapid and direct convergence with increasing M. For the ASYNNNI model, the strip leading to the transfer matrix and the associated direction of transfer are indicated in Fig. 1(b). The interactions are translationally invariant only over two (not one) lattice spacings in this direction. Therefore a product of two distinct transfer matrices should be used, as in the case of a modulated model.[41] For the OrthoII ground state to be consistent with the periodic boundary conditions, strip widths M should be multiples of 4. Within a column, the interactions are symmetric with respect to translation of two lattice sites along the column ($\underline{P}$) and reflection about a copper ion ($\underline{R}$).

For a system in the thermodynamic limit, the free energy can be conveniently represented by the logarithm of the largest eigenvalue of the transfer matrix. The degeneracy of the leading eigenvalues indicates a symmetry breaking associated with a phase transition. For a finite system, the leading eigenvalue is always nondegenerate. It is convenient (and greatly reduces the size of the transfer matrix) to separate all the eigenvalues into different symmetry classes according to the symmetry of their corresponding eigenvectors. The largest of those eigenvalues whose eigenvectors have both $\underline{P}$ and $\underline{R}$ symmetry is denoted as λ_0; the largest of those which breaks $\underline{R}$ symmetry, which is associated with orthorhombic symmetry breaking, is labeled λ_r. The largest eigenvalue which breaks $\underline{P}$ symmetry is labeled λ_t. In this system, the largest eigenvalue of the transfer matrix $\underline{T}$ is always λ_0. The close approach of λ_r or λ_t to λ_0 is the signature of a symmetry breaking. Finite-size-scaling theory predicts that when second-order phase transitions occur, the appropriate correlation length should grow linearly with strip width M,[42,43] for sufficiently large M. Thus, one expects

$$\xi_{r,M}^{-1} = \ln\left(\frac{\lambda_{0,M}}{\lambda_{r,M}}\right) \sim 1/M \tag{3}$$

for the Tetra-OrthoI transition, which breaks rotational

TABLE I. Interaction constants, in the Ising formulation, used in the phase diagram calculations, including the "canonical" values, the previous first-principles values of Refs. 31 and 32, the present first-principles values of Ref. 33, and those obtained by χ^2 fitting to experimental data in Poulsen *et al.* (Ref. 12), Fiig *et al.* (Ref. 17), and Hilton *et al.* (Ref. 14). Errors in fitting are not indicated.

Parameter set	V_1 (mRy)	V_2 (mRy)	V_3 (mRy)
"Canonical" (Ref. 6)	> 0	$-0.5V_1$	$0.5V_1$
Old first-principles (Refs. 31, 32)	6.9	−2.4	1.1
Present first-principles (Ref. 33)	6.71	−5.58	0.73
Poulsen *et al.* (Ref. 12)	6.81	−2.45	0.82
Fiig *et al.* (Ref. 17)	8.58	−3.09	1.03
Hilton *et al.* (Ref. 14)	4.4	−3.77	0.428

and reflectional ($4mm$) symmetry, and

$$\xi_{t,M}^{-1} = \ln\left(\frac{\lambda_{0,M}}{\lambda_{t,M}}\right) \sim 1/M \tag{4}$$

at the OrthoI-OrthoII phase transition, which breaks translational symmetry. Both these transitions involve the breaking of twofold degeneracy and correspondingly are in the Ising universality class. At the Tetra-OrthoII transition, both symmetries are broken simultaneously, with critical behavior associated with the class of XY models with cubic anisotropy. For finite strips, the rotational/reflectional breaking transition will precede the translation breaking transition as temperature is lowered, but as M increases the transitions will approach each other.

Each phase boundary was obtained by using Eqs. (3) and (4) for two different strip sizes M and $N = M+4$ and finding where $\xi_M/M = \xi_N/N$. To make the computer calculation of eigenvalues of the transfer matrix for large M possible, we follow the symmetry reduction method of Runnels and Combs[44] by dividing all 2^M configuration ψ_j's into disjoint equivalence classes $K_1, K_2, \ldots$. States in a given equivalence class are related through the $\underline{P}$ or the $\underline{R}$ operation. To calculate the largest eigenvalue λ_0, we define the equivalence class by both $\underline{P}$ and $\underline{R}$. The reduced matrix $\underline{S}$ defined by

$$S_{\alpha\beta} = \sum_{\psi_j \in K_\beta} T_{ij} \qquad (\psi_i \in K_\alpha) \tag{5}$$

will give all the eigenvalues satisfying $\underline{P}x = x$ and $\underline{R}x = x$. Here the Greek letters denote equivalence classes. Other definitions of the reduced matrix give eigenvalues satisfying different symmetries. Thus we can greatly reduce the size of the matrix. For example, in order to find the three largest eigenvalues for a transfer matrix with $M = 8$, we need to consider matrices of dimension no greater than 43×43. The eigenvalues are obtained numerically by applying the QR algorithm after reducing the matrix to Hessenberg form.[45]

IV. RESULTS AND DISCUSSION

The interaction parameters used here are based on first-principles linear muffin tin orbital (LMTO) electronic structure calculations and were obtained from the calculated total energies using the Connolly-Williams method.[46] The present EPI's (Ref. 33) differ slightly from those previously published[31,32] and are based on a more highly converged set of electronic structure calculations and on a different set of ordered structures which spans only the region $6.0 \leq z \leq 7.0$. Further details on these calculations and the ensuing parameters will be given elsewhere.[33] Table I lists the values of the various interaction parameter sets considered here. All of these values obey the inequalities set out in Ref. 5 and therefore support the stability of OrthoI and OrthoII as ground states.

For the ASYNNNI model with the present EPI's and no interaction beyond NNN, the T-c phase diagram is shown in Fig. 2. The solid line is generated by scaling of strips with widths of 8 and 12 and the dashed line is generated by scaling of strips with widths of 4 and 8 to assess the finite-size effect. Previous work[8,10] has shown only a small deviation of the phase boundary between 8-12 scaling and 12-16 scaling at most temperatures and throughout the concentration region. Therefore 8-12 scaling is believed to be sufficient to determine the phase boundary. The topology of this diagram is very similar to that determined for other values of the EPI's.[8,10,14,17] The main difference is that the Tetra-OrthoI line and the OrthoI-OrthoII line never meet (although their extrapolations, with larger matrices, might). These results allow for the possibility that a sample preparation pro-

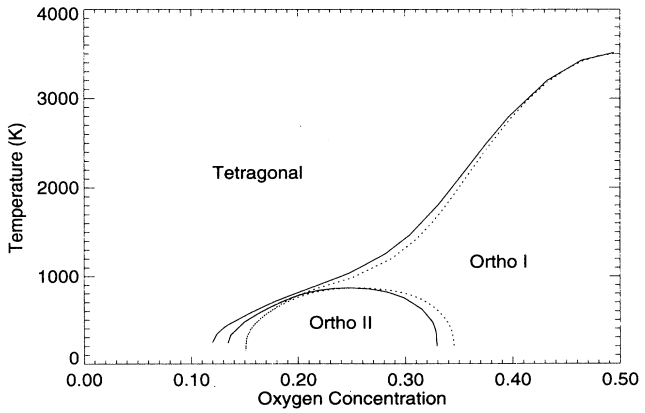

FIG. 2. Temperature-concentration phase diagram calculated from transfer-matrix finite-size scaling using the present first-principles interaction parameters. Solid lines: 8-12 scaling; dotted lines: 4-8 scaling.

cess consisting of annealing at constant chemical potential (i.e., constant oxygen partial pressure) passes from the Tetra phase through a narrow region of OrthoI into the OrthoII field and finally into the high-concentration OrthoI region. However, the ASYNNNI model is less appropriate at low concentrations because of depletion of the apical oxygen sites, and therefore this effect may not be experimentally observable. Moreover, sample equilibration at low temperatures is very hard to accomplish, exacerbating the difficulty of observing a Tetra-OrthoI-OrthoII transition sequence.

To illustrate the effects of various choices for the EPI's, in Fig. 3 we compare the phase diagrams computed by the TMFSS method for the present first-principles parameters and for the "canonical" parameters with $V_3 = -V_2 = (1/2)V_1$ as used in previous studies.[8,10] The most significant effects are the possible disappearance of the intersection (4-state Potts[8]) point, a slight lowering of the top of the OrthoII stability region, and a broadening of the OrthoII phase field. This can be readily understood if one realizes that for the present parameters the ratio $|V_2/V_1| = 0.83$ is substantially larger than for the canonical values, while the ratio $V_3/V_1 = 0.11$ is considerably less than in the canonical case. Thus the EPI responsible for holding the chains together is much larger than first estimated, while that responsible for interchain repulsion is weaker. Note that the temperature scale in this figure is in units of k_BT/V_1, and therefore shifts on this temperature scale do not necessarily correspond to a shift in absolute temperature.

Figure 4 compares the phase diagram computed from the first-principles parameters with experimental data.[14,32] Most of these measurements are for the OrthoI-Tetra transition line. Schwarz *et al.*[47] have argued that the top of the OrthoII stability region should be near 420 K, considerably lower than in the old first-principles calculations[9,14,31,32] which put it near 600 K. The present parameters extend this region to even higher temperatures. In fact, whereas the old first-principles EPI's led to a phase diagram for which the OrthoI-Tetra line was too low, the present parameters, based on improved elec-

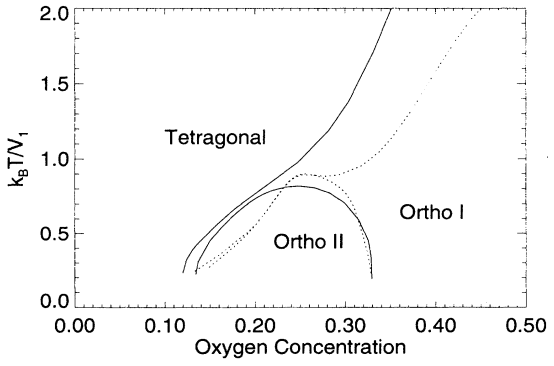

FIG. 3. Comparison of phase diagrams obtained using different interactions. Solid lines represent the phase boundary for the first-principles interactions, and the dotted lines represent the canonical interactions with $V_2 = -V_3 = -(1/2)V_1$. The phase diagrams are obtained by 8-12 scaling for both cases.

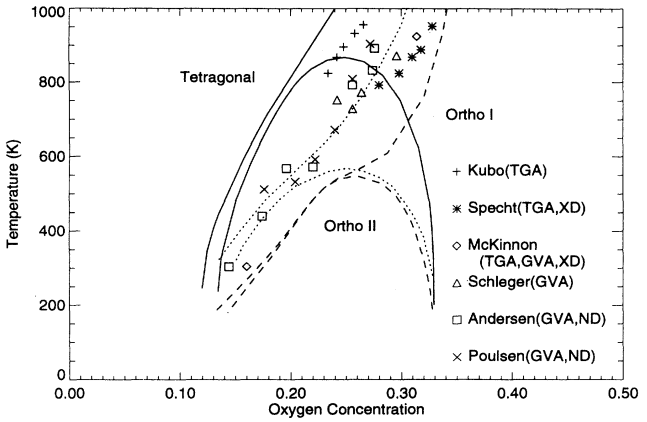

FIG. 4. Comparison between the calculated phase diagrams and experiment. Solid lines are obtained using the present first-principles interactions (Ref. 33) and the dashed lines by the previous first-principles interactions (Refs. 31, 32). Also the phase boundary using interactions from χ^2 fits to experimental data (Ref. 14) is shown here, as represented by dotted lines. The experimental data points, the surnames of the first author, and the initials of the measurement techniques are taken from Ref. 14 and references therein.

tronic structure calculations, overestimate the upwards shift of this transition line, as well as the extent of the OrthoII region. Nevertheless, the current phase diagram fits the experimental values quite well, especially since no adjustable parameters were used. The discrepancies are most probably caused by physical factors which are not taken into account in the ASYNNNI model, for example, elastic effects, weak long-range interactions, and interactions in the z-axis direction of the unit cell.

Figure 4 also shows the phase diagram obtained by Hilton *et al.* using transfer-matrix finite-size scaling.[14] These authors fitted the V_1, V_2, and V_3 interactions to experimental data and naturally get a very good agreement between theory and experiment, which can be taken as a justification of the underlying assumptions of the ASYNNNI model. Moreover, a comparison of the parameters obtained by Hilton *et al.* and the present first-principles values allows us to identify those contributions to the Hamiltonian that are essentially electronic in origin (and therefore contained in the first-principles EPI's) and those for which a different mechanism must be invoked. The parameters obtained by Hilton *et al.* are a synthesis of electronic structure contributions and other physical effects not included in the first-principles calculations. In this way, physical effects which are not readily represented within the electronic structure calculations renormalize the values of the fitted parameters, accounting for much of the observed difference between the first-principles results and the experimental data. However, the generally strong correspondence between the experimental data and the phase diagram calculated from the ASYNNNI model with first-principles interactions demonstrates that the dominant effects are already well treated, and that the contribution of effects omitted from the electronic structure calculations and from the

Hamiltonian is relatively minor. Note that the signs of the interaction parameters were not constrained in the Connolly-Williams fit to the calculated total energies, so the observed physical region of parameter space for the observed orthorhombic phases is already a consequence of the electronic structure.

As listed in Table I, the present first-principles calculations yield an increased magnitude for V_2 compared to the old values, in the same direction as Hilton *et al.* indicate, although the increase in magnitude is larger than needed to provide an optimal fit to experiment. Likewise, the V_3 interaction is decreased in magnitude, again in the same direction indicated by the least-squares fit. The largest difference between Hilton *et al.*'s fit and the first-principles EPI's is in the NN parameter V_1. The value needed for an optimal fit is almost 35% less than that obtained from the electronic structure determination. This is a significant difference that cannot be attributed to uncertainties in the Connolly-Williams method or approximations in the band structure calculations, such as the local density approximation and others. Thus, this discrepancy must be attributed to effects that are not included in the calculations, most likely elastic in origin. It is also worth pointing out that the interactions fitted by Hilton *et al.* are restricted to a rather narrow concentration range ($0.15 < c < 0.30$) because experiments have only measured the transition points in this domain, whereas those obtained by first-principles stretch across the entire region $0.0 \leq c \leq 0.5$. We note that all of the statistical mechanical treatments neglect a number of contributions to the free energy, such as vibrational entropy. However, these are expected to have only a minor effect on the phase diagram, although they may become important for comparison with experimentally measured thermodynamic functions, such as specific heat.

Poulsen *et al.*[12] and Fiig *et al.*[17] also determined a set of EPI's based on a fit to experimental data. The parameters they obtained were in good agreement with the old first-principles values,[31,32] but differed significantly from the results of Hilton *et al.* This is indicative of the uncertainties involved in extracting a set of EPI's from experimental data, as it is possible that several different parameter sets could result in equally good fits. In view of this, the differences between the experimental EPI's obtained by Hilton *et al.* and the present first-principles values may not be all that significant. However, since the parameter set of Hilton *et al.* is based on a larger set of experimental data, we prefer to use their EPI's as a reference for the experimental parameters.

In order to investigate the contribution that each NNN interaction separately makes to the phase diagram, Fig. 5 gives an indication of how much the phase boundaries change as each interaction is modified individually. The dotted lines represent the calculated boundaries when V_2 is replaced by $V_2' = V_2/1.1$, while the dashed lines show the effects of replacing V_3 by $V_3' = 1.5V_3$. The observed shifts may be interpreted as follows. The attractive V_2 interaction favors oxygen atoms forming O-Cu-O chains; therefore the Tetra-OrthoI and the OrthoI-OrthoII transition temperatures increase as the attraction becomes stronger. In the high-oxygen-content region, a stronger repulsive V_3 makes the OrthoI phase relatively less favorable than the Tetra phase by increasing the repulsion between adjacent Cu-O chains; at low oxygen content, it correspondingly makes the OrthoII phase more favorable. Therefore, as shown in Fig. 5, a stronger V_3 raises the OrthoI-OrthoII transition temperature but lowers the Tetra-OrthoI transition temperature slightly in the high-oxygen-content region. These trends are consistent with those observed in Figs. 3 and 4, but since in those cases all parameters were allowed to change simultaneously, the various contributions are hard to resolve. Compatibility with the measurements of Schwarz *et al.*,[47] who find that the OrthoII phase disappears at temperatures above 420 K, could be achieved by a major decrease of $|V_2|$; however, that would shift the OrthoI-Tetra boundary line, and it is not clear that V_1 and V_3 can be adjusted sufficiently to retain the good agreement between theory and experiment for that transition line. Alternatively, a reduction of V_3 also tends to destabilize the OrthoII phase. In any case, even the fitted parameters of Hilton *et al.* put the OrthoII region considerably higher than permitted by the results of Schwarz *et al.* Further experimental study of this issue would be useful. Table II lists the shifts of the various phase transition temperatures when either V_2 or V_3 is varied slightly about its "present first-principles" value in Table I, with c fixed at 0.25.

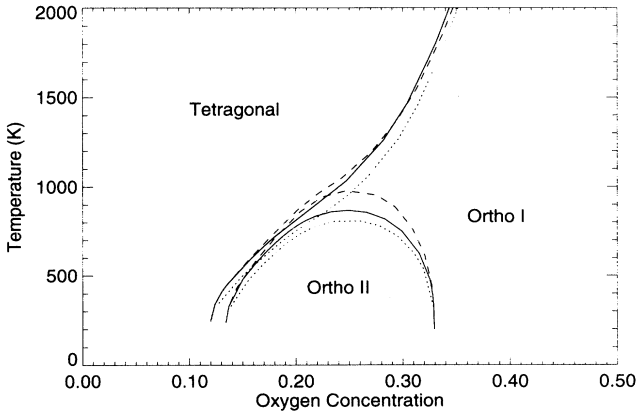

FIG. 5. Sensitivity of the phase boundary to the change of interaction value. Solid lines represent the first-principles interactions; the dotted lines represent the shift of the boundary when $V_2' = V_2/1.1$; and the dashed lines represent the shift when $V_3' = 1.5V_3$. In each case, only one interaction is changed to the primed value, while the rest are fixed at the first-principles values.

TABLE II. Incremental variations ($\Delta T_c/\Delta|V_i|$) of the transition temperatures due to modifications of interaction constants. The basal plane oxygen concentration is fixed at $c = 0.25$ and the phase boundaries are evaluated by 8-12 scaling. Positive values indicate that T_c increases as the interactions increase in absolute value.

Interaction modified	Tetra-OrthoI (K/mRy)	Tetra-OrthoII (K/mRy)
V_2	175	110
V_3	66.5	352

The first-principles electronic structure calculations also yield values for longer-range interactions,[33] though their magnitude is smaller than those in the usual parameter set. The transfer-matrix method has difficulties in dealing with long-range interactions in general, as do most other phase diagram calculation methods. If we include long-range interactions between nearest-neighbor columns only, we will break the rotational symmetry of the square lattice and its effect is hard to evaluate. But at low temperature, i.e., $k_BT < 0.2V_1$, the oxygen atoms are very unlikely to form a nearest-neighbor pair; therefore we can consider the nearest-neighbor interaction by an exclusion and reduce the number of permissible states. To make the calculations feasible, we first approximate V_1 by an exclusion, which only shifts (to lower concentration) the high-temperature Tetra-OrthoI boundary, but hardly has any effect at low-temperatures. Subsequent inclusion of the third-neighbor interaction V_4 has minimal effect. We show in Fig. 6 that, in the low-temperature region, the phase diagram obtained by taking V_1 as an exclusion is almost indistinguishable from that obtained with a finite V_1. Thus, we can include a third-nearest-neighbor interaction V_4 without a formidable increase in computer time. Figure 6 shows the T-c diagram with $V_4 = 0$ and $V_4 = 0.05$ mRy. As can be seen, the inclusion of this longer-range interaction does not change the phase diagram significantly. Like V_3, this interaction also makes OrthoI less favorable with respect to OrthoII at low oxygen content and raises the OrthoI-OrthoII transition temperature.

Other authors have also considered the effects of adding another more-distant-neighbor interaction to the ASYNNNI Hamiltonian, although these are typically viewed as interactions between parallel chains. Günther *et al.*[26] invoke a weakly attractive "ϕ_{CC}" between alternate-spacing (OrthoII-like) chains to produce a first-order transition between OrthoI and OrthoII as observed in a number of experiments.[26,28] This interaction is actually between seventh neighbors, although it is the second shortest "through-copper" bond. In order to keep the size of the transfer matrix manageable, only the subset of such bonds that connect adjacent strips was retained. Ceder *et al.*[48] added to the ASYNNNI model a repulsive interaction between alternately spaced chains along a V_3 bond, but twice its length, which stabilizes a triple-cell chain phase OrthoIII. This fifth-neighbor interaction was also called V_4, but should not be confused with the V_4 interaction in this paper. In addition they considered the effects of out-of-plane interactions to make the calculations feasible within the CVM. They treated V_1 as an exclusion, an excellent approximation at low temperature, and found first-order transitions between OrthoIII and the other orthorhombic phases.[49] Rather than introducing out-of-plane interactions, Zubkus *et al.*[50] obtained similar results by adding long-range attractive interactions to stabilize the OrthoIII phase. These interactions were taken into account via a mean-field approximation, amounting to a concentration-dependent shift in the chemical potential. Their calculated phase diagram exhibits coexistence regions between all three orthorhombic phases. However, there is as yet no experimental evidence to support these results.

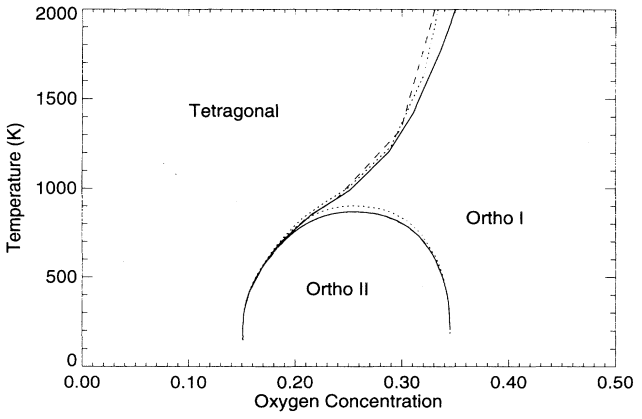

FIG. 6. Estimation of the effect of the third-NN interaction V_4. Solid lines represent the phase boundary for the first-principles interactions with finite V_1 and no V_4; the dashed line is obtained by making V_1 infinite. One can note that at low temperatures the phase boundary is indistinguishable from the original one (with finite V_1). At high temperatures, of course, treating V_1 as an exclusion will produce a major shift in the OrthoI-Tetra phase boundary. The dotted lines represent the phase boundary with infinite V_1 and $V_4 =$ 0.05 mRy.

V. CONCLUSIONS

Starting from first-principles calculations of the interactions responsible for oxygen ordering in $YBa_2Cu_3O_z$ within the ASYNNNI model, we have obtained a structural phase diagram that shows satisfactory agreement with experimental results. This model clearly includes much of the important physics in the real system. The remaining *qualitative* discrepancies must be attributed to physical effects not incorporated into the two-dimensional lattice model, such as elasticity, further-neighbor interactions, and three-dimensional interactions along the z axis. The *quantitative* discrepancies between theory and experiment must be traced back to effects that are not included in the electronic structure calculations which form the basis for the calculated EPI's and, to a lesser extent, to approximations inherent in the statistical mechanical treatment.

A quantitative comparison between the first-principles phase diagram and experiment is aided by the work of Hilton *et al.*,[14] who determined a set of V_1, V_2, and V_3 interactions that best describe the experimental phase boundary. A comparison between those EPI's and the first-principles ones permits one to attribute any differences to effects not contained in the electronic structure calculations, with most likely elastic strain energies as the dominant factor. One may conclude that strain will tend to diminish all interactions in magnitude (see Table I). There is reason to believe that this is true at least for the V_1 interaction, so the present first-principles values are expected to overestimate the magnitude of this parameter.[33] This suggests that the values determined by Hilton *et al.* are a better representation of experiment

than the other empirically derived parameter sets.[12,17] Unfortunately, the values determined by Hilton *et al.* did not include the more recent finding[47] that the OrthoII phase boundary region peaks at lower temperatures than was hitherto believed. It would be very interesting to see if this discovery has a major impact on the best-fit parameters, or might even necessitate a revision of the ASYNNNI model itself. Strain energies have recently been included in empirical ways in lattice-gas models for $YBa_2Cu_3O_z$ (Refs. 29, 30, and 40) and bear further investigation.

Elastic effects are probably also responsible for the experimentally observed $\sqrt{2}$ structures,[34,35] so these phases are not likely to be stable ground states of a static-lattice Hamiltonian. No first-order transitions exist within the ASYNNNI model using parameters that stabilize OrthoI and OrthoII, but they also may be caused by elastic effects.[28] Modulated superstructures consisting of chain-ordered phases beyond OrthoI and OrthoII are not stable within the ASYNNNI model but become so upon the addition of further-neighbor interactions.[23,24,38,39] Weak repulsive interactions are compatible with the LMTO results and hardly affect the main phase boundaries, but they do produce narrow stability regions for the modulated phases.

The quantitative differences between the first-principles parameters and the empirical parameter sets may well be due to a renormalization of the first-principles EPI's due to elastic and other effects. However, the actual strength of such a renormalization is still in question due to uncertainties in the determination of empirical parameter values. The calculations presented here demonstrate that it is difficult to identify characteristic phase diagram features that are associated with a single interaction parameter. All the features in the phase diagram are altered when a single parameter is varied (see Fig. 5), so the problem of determining a good fit to experimental data becomes more challenging. This inversion procedure may well be ill posed so its ability to provide a unique set of parameters is in doubt. Nevertheless, the calculations do suggest that some renormalization of the first-principles EPI's is in order, since an accurate phase diagram calculation based on the best available theoretical parameters still yields phase boundaries slightly higher than experiment. Further analysis of the experimental data and the stability and uniqueness of the empirically derived parameters would be very helpful in resolving this issue.

ACKNOWLEDGMENTS

D.J.L. and T.L.E. were supported in part by NSF-MRG Grant No. DMR 91-03031. P.A.S.'s work was performed under the auspices of the U.S. Department of Energy by Lawrence Livermore National Laboratory under Contract No. W-7405-ENG-48.

[1] W. Hayes and A. M. Stoneham, *Defects and Defect Processes in Nonmetallic Solids* (Wiley, New York, 1985).
[2] R. Beyers and T. M. Shaw, Solid State Phys. **42**, 135 (1989).
[3] B. W. Veal, A. P. Paulikas, H. You, H. Shi, Y. Fang, and J. W. Downey, Phys. Rev. B **42**, 6305 (1990).
[4] D. de Fontaine, L. T. Wille, and S. C. Moss, Phys. Rev. B **36**, 5709 (1987).
[5] L. T. Wille and D. de Fontaine, Phys. Rev. B **37**, 2227 (1988).
[6] L. T. Wille, A. Berera, and D. de Fontaine, Phys. Rev. Lett. **60**, 1065 (1988).
[7] R. Kikuchi and J. S. Choi, Physica C **160**, 347 (1989).
[8] N. C. Bartelt, T. L. Einstein, and L. T. Wille, Phys. Rev. B **40**, 10 759 (1989).
[9] G. Ceder, M. Asta, W. C. Carter, M. Kraitchman, D. de Fontaine, M. E. Mann, and M. Sluiter, Phys. Rev. B **41**, 8698 (1990).
[10] T. Aukrust, M. A. Novotny, P. A. Rikvold, and D. P. Landau, Phys. Rev. B **41**, 8772 (1990).
[11] J. V. Andersen, H. Bohr, and O. G. Mouritsen, Phys. Rev. B **42**, 283 (1990).
[12] H. F. Poulsen, N. H. Andersen, J. V. Andersen, H. Bohr, and O. G. Mouritsen, Phys. Rev. Lett. **66**, 465 (1991).
[13] V. E. Zubkus, E. E. Tornau, S. Lapinskas, and P. J. Kundrotas, Phys. Rev. B **43**, 13 112 (1991).
[14] D. K. Hilton, B. M. Gorman, P. A. Rikvold, and M. A. Novotny, Phys. Rev. B **46**, 381 (1992), and references therein.
[15] V. M. Matic, Physica A **184**, 571 (1992).
[16] W. Selke and G. V. Uimin, Physica C **214**, 37 (1993).
[17] T. Fiig, J. V. Andersen, N. H. Andersen, P. A. Lindgård, O. G. Mouritsen, and H. F. Poulsen, Physica C **217**, 34 (1993).
[18] J. Oitmaa, Y. Jie, and L. T. Wille, J. Phys. Condens. Matter **5**, 4161 (1993).
[19] G. Uimin, Phys. Rev. B **50**, 9531 (1994).
[20] H. Shaked, J. D. Jorgensen, B. A. Hunter, R. L. Hitterman, A. P. Paulikas, and B. W. Veal, Phys. Rev. B **51**, 547 (1995), and references therein.
[21] P. Schleger, W. N. Hardy, and H. Casalta, Phys. Rev. B **49**, 514 (1994).
[22] R. Tétot, C. Giaconia, A. Finel, and G. Boureau, Phys. Rev. B **48**, 10 090 (1993).
[23] D. de Fontaine, G. Ceder, and M. Asta, Nature **343**, 544 (1990).
[24] D. Adelman, C. P. Burmester, L. T. Wille, P. A. Sterne, and R. Gronsky, J. Phys. Condens. Matter **4**, L585 (1992).
[25] R. Beyers, B. T. Ahn, G. Gorman, V. Y. Lee, S. S. P. Parkin, M. L. Ramirez, K. P. Roche, J. E. Vazquez, T. M. Gür, and R. A. Huggins, Nature **340**, 619 (1989).
[26] C. C. A. Günther, P. A. Rikvold, and M. A. Novotny, Phys. Rev. B **42**, 10 738 (1990).
[27] J. M. Sanchez and J. L. Morán-López, Solid State Commun. **79**, 151 (1991).
[28] K. B. Blagoev and L. T. Wille, Phys. Rev. B **48**, 6588

(1993).
[29] M. Goldman, C. P. Burmester, L. T. Wille, and R. Gronsky, Phys. Rev. B **50**, 1337 (1994).
[30] M. Goldman, C. P. Burmester, L. T. Wille, and R. Gronsky, Philos. Mag. Lett. **70**, 65 (1994).
[31] P. A. Sterne and L. T. Wille, Physica C **162**, 223 (1989).
[32] P. A. Sterne and L. T. Wille, in *Atomic Scale Calculations of Structure in Materials*, edited by M. S. Daw and M. A. Schlüter, MRS Symposia Proceedings No. 193 (Materials Research Society, Pittsburgh, 1990), p. 35.
[33] P. A. Sterne and L. T. Wille (unpublished).
[34] T. Krekels, T. S. Shi, J. Reyes-Gasga, G. Van Tendeloo, J. Van Landuyt, and S. Amelinckx, Physica C **167**, 677 (1990), and references therein.
[35] R. Sonntag, D. Hohlwein, T. Brückel, and G. Collin, Phys. Rev. Lett. **66**, 1497 (1991).
[36] A. G. Khachaturyan and J. W. Morris, Jr., Phys. Rev. Lett. **59**, 2776 (1987).
[37] A. G. Khachaturyan and J. W. Morris, Jr., Phys. Rev. Lett. **61**, 215 (1988).
[38] A. A. Aligia and J. Garcés, Phys. Rev. B **49**, 524 (1994), and references therein.
[39] A. A. Aligia, J. Garcés, and J. P. Abriata, Physica C **221**, 109 (1994), and references therein.
[40] S. Semenovskaya and A. G. Khachaturyan, Phys. Rev. B **46**, 6511 (1992).
[41] Translational invariance over one lattice spacing could easily be regained by rotating the transfer direction by 45°, while keeping the strip direction the same so that all the ASYNNNI interactions can be simply incorporated by a pair of neighboring strips so that one of the two OrthoI orientations is not favored. The two approaches require roughly comparable computer usage, but the symmetry analysis is easier when the transfer direction is perpendicular to the strip. See Refs. 8 and 10.
[42] M. P. Nightingale, J. Appl. Phys. **53**, 7927 (1982).
[43] M. N. Barber, in *Phase Transitions and Critical Phenomena*, edited by C. Domb and J. L. Lebowitz (Academic, New York, 1987), Vol. 8, p. 145.
[44] L. K. Runnels and L. L. Combs, J. Chem. Phys. **45**, 2482 (1966).
[45] W. H. Press, S. A. Teukolsky, W. T. Vetterling, and B. P. Flannery, *Numerical Recipes in FORTRAN: the Art of Scientific Computing*, 2nd ed. (Cambridge University Press, Cambridge, England, 1992); specifically, we used NAG's hqr routine.
[46] J. W. D. Connolly and A. R. Williams, Phys. Rev. B **27**, 5169 (1983).
[47] W. Schwarz, O. Blaschko, G. Collin, and F. Marucco, Phys. Rev. B **48**, 6513 (1993).
[48] G. Ceder, M. Asta, and D. de Fontaine, Physica C **177**, 106 (1991).
[49] Note that the V_4 used in the present work does not destabilize the OrthoII phase, nor does it introduce any current ground states.
[50] V. E. Zubkus, S. Lapinskas, A. Rosengren, and E. E. Tornau, Physica C **206**, 155 (1993).